Second-order nonlinear optical susceptibility of asymmetric quantum wells

R. Atanasov and F. Bassani
Scuola Normale Superiore, Piazza dei Cavalieri 7, I-56126 Pisa, Italy

V.M. Agranovich
Institute of Spectroscopy Russian Academy of Science, Troitsk, Moscow, Russia
(Received 22 February 1994)

We give a detailed procedure for the calculation of the second-harmonic-generation susceptibility tensor in single and multiple asymmetric quantum wells (AQW's). The effect of nonhomogeneity is explicitly included. Exciton states and continuum states are considered. The contributions due to the asymmetry of the confining potential and to the inversion asymmetry of the bulk material are separately assessed. Numerical calculations are carried out for two typical AQW's of $GaAs/Ga_{1-x}Al_xAs$. The results indicate larger values than in the bulk, in agreement with preliminary experimental data.

I. INTRODUCTION

Nonlinear optical properties of quantum wells (QW's) are of interest because of their relevance for studying practical applications and as a probe for the electronic structure of mesoscopic media. In particular, it has been shown that asymmetric quantum wells (AQW's) display very large second-order[1–17] and third-order[18–22] susceptibilities.

In the present work, we consider the optical second-order susceptibility $\chi^{(2)}$ of asymmetric quantum wells and examine in detail two contributions: one due to the absence of inversion symmetry as in the bulk and the other to the absence of specular symmetry of the AQW confining potential. In general, the existing theoretical and experimental studies can be divided into two groups, depending on the light frequency: those which have photon energy in the region of intraband (intersubband) transitions (near infrared) and a second group dealing with energies in the region of interband (valence to conduction band) transitions (visible light).

In the region of intraband transitions ($\lambda = 9 - 11\,\mu$m), one deals with n-doped AQW's with a concentration of electrons n_c in the conduction band. Due to the symmetry of the electronic states, the only nonzero element of the quadratic nonlinear optical susceptibility is $\chi^{(2)}_{zzz}$ or simply $\chi^{(2)}$. Depending on the material, the shape of the AQW, and n_c, the modulus of $\chi^{(2)}$ can reach extremely large values in comparison with $|\chi^{(2)}(0,0)|$ of bulk GaAs, which has been found to be about 1.8×10^{-10} m/V.[23–26] In different samples of $GaAs/Ga_xAl_{1-x}As$ AQW's, peaks of $|\chi^{(2)}|$ reach values of the order of 5×10^{-7} m/V.[1–4] In $Al_xIn_{1-x}As/Ga_yIn_{1-y}As$ AQW's, Sirtori *et al.*[7,8] observed a peak $|\chi^{(2)}|$ of approximately 5×10^{-8} m/V. Similar values are obtained in electric-field-biased symmetric quantum wells (SQW's). For example, Fejer *et al.*[9] observed peak values of $\chi^{(2)}$ equal to 2.8×10^{-8} m/V in GaAs SQW's under an electric field of 36 kV/cm. The theory based on intraband (intersubband) transitions accounts for these findings.[1,2,7]

Differently from the case considered above, the second-order optical susceptibility studied in the interband transition region has received very little attention. Tsang *et al.*[10,11] have calculated $\chi^{(2)}_{xzx}(\omega,\omega)$ of an electric-field-biased SQW. They consider exciton and continuum states and conclude that the exciton states contribute only 30% of the total $\chi^{(2)}_{xzx}$ and peak values of the order of 3×10^{-11} m/V result.[10] Asymmetric QW's have been considered by Kurgin,[12,13] without inclusion of exciton states. In the case of an optimized double $GaAs/Ga_{1-x}Al_xAs$ AQW, he obtains a maximum value of $|\chi^{(2)}_{xzx}(\omega,\omega)| \approx 1.8\times10^{-12}$ m/V.[13] For a similar sample with multiple AQW, experiments of Xie *et al.*[14] give peak values of approximately 8×10^{-9} m/V, over three orders of magnitude larger, and still one order of magnitude larger than obtained in recent calculations by Harshman and Wang.[15] Scandolo *et al.*[16] have proposed a steplike GaSb/InAsSb AQW for efficient second-harmonic generation, with an expected second-harmonic coefficient about 60 times greater than that of the bulk GaAs.

In the present work, we address the problem of second-harmonic generation in an AQW in the region of interband transitions including exciton effects (exciton region). Our purpose is threefold: first, to calculate all the nonzero components of $\chi^{(2)}$ making use of the density matrix approach[27,28] in the electric dipole approximation; second, to calculate $\chi^{(2)}$, taking into account the nonlocal nature of the AQW response to the electric field; and third, to consider the contribution of the bulklike inversion asymmetry previously neglected. We perform these calculations in an averaged field approximation proposed by Agranovich,[29] and applied to the linear optical properties of superlattices[30,31] and AQW's.[32] This method is based on the fact that the radiation wavelength λ is large compared with the period L of a multiple AQW with quantum well length L_w and barrier length

L_B, i.e., $\lambda \gg L = L_w + L_B$. In this case we use unretarded ($c \to \infty$) Maxwell equations and perform self-consistent calculations to obtain the field distribution inside the well, as well as the optical response. The internal electric field distribution is determined by the inhomogeneous charge distribution and the dielectric mismatch.[32]

In Sec. II we recast the general density matrix formalism for the second-order nonlinear optical susceptibility, making use of the exciton states and continuum states of an AQW. The discussion of the dipole matrix element calculation is given in Sec. III. In Sec. IV we calculate the tensor $\chi^{(2)}(\omega,\omega)$ in the electric dipole approximation and local response approach. In Sec. V we derive an averaged quadratic susceptibility tensor $\overline{\chi}^{(2)}$ including nonlocal response effects and report some numerical calculations. The main results are discussed in Sec. VI.

II. SECOND-ORDER SUSCEPTIBILITIES IN BULK AND IN QUANTUM WELLS

The local quadratic polarization $\boldsymbol{P}^{(2)}(t,\boldsymbol{r})$ of a medium interacting with an external electric field $\boldsymbol{E}(t,\boldsymbol{r})$ may be expressed in the form[27,28]

$$P_p^{(2)}(t,\boldsymbol{r}) = \varepsilon_0 \int_{\tau_1}\int_{\tau_2}\int_{r_1}\int_{r_2} G_{pqr}^{(2)}(\boldsymbol{r},\tau_1,\tau_2,\boldsymbol{r}_1,\boldsymbol{r}_2) \times E_q(t-\tau_1,\boldsymbol{r}_1)E_r(t-\tau_2,\boldsymbol{r}_2), \quad (1)$$

where ε_0 is the permittivity of free space and $G_{pqr}^{(2)}$ denotes the quadratic response function. The subscripts p,q,r label the Cartesian coordinates and a double repeated subscript means summation over all the coordinates. The integration over τ_1 and τ_2 is performed in the infinite interval $(-\infty,\infty)$ and the integration over $\boldsymbol{r}_1$ and $\boldsymbol{r}_2$ in the volume V of the sample. The time dependence of $G^{(2)}$ is known as temporal dispersion,[27,28] and causality implies that $G_{pqr}^{(2)} = 0$ when τ_1 or τ_2 is negative. The space dependence is usually neglected in the second-order optical susceptibilities of AQW's, but will be considered in the following analysis.

A. Temporal dispersion

We first consider the time dependence in a homogeneous medium and neglect spatial dispersion in the calculation of $\chi^{(2)}$. We consider a fully local response of the medium, so that, taking the electric field as a superposition of two monochromatic waves of frequencies ω_1 and ω_2, we obtain

$$P_p^{(2)}(\Omega) = \varepsilon_0 \Upsilon \chi_{pqr}^{(2)}(\omega_1,\omega_2)E_q(\omega_1)E_r(\omega_2). \quad (2)$$

Here $\Omega = \omega_1 + \omega_2$ and the tensor $\chi^{(2)}$ is the quadratic nonlinear optical susceptibility, Υ being a number which accounts for the possible permutations of indices. According to the type of nonlinear process,[27] the frequencies ω_1 and ω_2 can be taken to be positive or negative to describe different nonlinear processes; for example, second harmonic generation occurs when $\omega_1 = \omega_2$ and $\Upsilon = 1/2$; optical rectification when $\omega_1 = -\omega_2$, and $\Upsilon = 1/2$; and the Pockels effect (when $\omega_1 = 0$, $\omega_2 \neq 0$, and $\Upsilon = 1/2$). Equation (2) gives the definition of quadratic optical susceptibility with temporal dispersion. In the dipole approximation, the density matrix approach gives a very general expression[27,28] for $\chi^{(2)}$ in terms of the eigenstates of the medium under consideration

$$\chi_{pqr}^{(2)}(\omega_1,\omega_2) = \frac{1+P_{12}}{2\varepsilon_0 V} \sum_{s_1,s_2,s_3} \frac{\langle s_1|d_p|s_2\rangle\langle s_2|d_q|s_3\rangle\langle s_3|d_r|s_1\rangle}{(\hbar\omega_1 + \hbar\omega_2 - E_{s_2 s_1})} \left[\frac{f(s_1)-f(s_3)}{\hbar\omega_2 - E_{s_3 s_1}} - \frac{f(s_3)-f(s_2)}{\hbar\omega_1 - E_{s_2 s_3}}\right], \quad (3)$$

where $E_{ss'} = E_s - E_{s'}$. Here s_1, s_2, and s_3 denote quantum numbers labeling the eigenfunctions $|s_i\rangle$ and the eigenvalues E_{s_i}, $f(s_i)$ is the Fermi distributions, d_p is the p-component of the dipole moment operator, and P_{12} is an operator which permutes the pairs (q,ω_1) and (r,ω_2). From Eq. (3) the basic intrinsic permutational symmetry $\chi_{pqr}^{(2)}(\omega_1,\omega_2) = \chi_{prq}^{(2)}(\omega_2,\omega_1)$ originates.

B. Nonlocal effects

The space dependence of the Green function in Eq. (1) takes into account the nonlocal nature in the optical response, whose main contribution is due to the nonhomogeneity of the medium under consideration. In the case of QW's the nonlocality influences the radiative and nonradiative quantum well polaritons, which can be computed taking into account the dielectric mismatch and the charge distribution inside the QW.[32] In order to include these factors in the calculation of nonlinear effects in quantum wells, we consider explicitly the space dependence of Eq. (1) in the growth direction and perform the integration in the plane of the well, which gives the usual conservation of the total in-plane momentum. Then, after a Fourier transformation on the time variables we obtain

$$P_p^{(2)}(\Omega,z) = \varepsilon_0 \Upsilon \int_0^L dz_1 \int_0^L dz_2\, \chi_{pqr}^{(2)}(\omega_1,\omega_2,z,z_1,z_2) \times E_q(\omega_1,z_1)E_r(\omega_2,z_2). \quad (4)$$

Here $\chi_{pqr}^{(2)}(\omega_1,\omega_2,z,z_1,z_2)$ is the nonlocal second-order susceptibility. It may be calculated making use of the density matrix approach, but the interaction Hamiltonian is to be taken in the form $-\int \boldsymbol{P}\cdot\boldsymbol{E}$ instead of the simpler form $-\boldsymbol{d}\cdot\boldsymbol{E}$ used in the case of temporal dispersion. Thus we obtain for the total polarization in a thickness L,

$$\int_0^L dz\, P_p^{(2)}(\Omega,z) = \varepsilon_0 \sum_{s_1,s_2,s_3} \Upsilon L_w \frac{1+P_{12}}{2\varepsilon_0 V_w(\hbar\Omega - E_{s_1 s})} \times \left[\frac{f(s_1)-f(s_3)}{\omega_2 - E_{s_3 s_1}} - \frac{f(s_3)-f(s_2)}{\omega_1 - E_{s_2 s_3}} \right] \langle s_1|d_p|s_2\rangle \times \langle s_2|d_q E_q|s_3\rangle \langle s_3|d_r E_r|s_1\rangle, \quad (5)$$

where we use the same notations as in Eq. (3). Maxwell equations relate averaged polarizations to averaged fields by means of the linear and nonlinear susceptibilities. To obtain these averaged quantities inside an AQW, we must calculate the polarization distribution $P(z)$ and the electric field which produces it. Here we can use the fact that the light wavelength λ is much greater than L_w. A similar situation appears in the case of multiple AQW's, when the period L is much smaller than λ. In both cases we can neglect the variation of the Maxwell fields inside the well and define averaged fields as

$$\overline{F_p} = \frac{1}{L}\int_0^L dz\, F_p(z) = \frac{1}{L}\langle F_p\rangle, \quad (6)$$

where $\boldsymbol{F}$ denotes the polarization, the electric field, or the electric displacement vector $\boldsymbol{D}$. We would like to emphasize that the integration in Eq. (6) is performed on one period L in case of multiple QW's and on the QW width L_w in the case of a single quantum well. We have described the consequence of the above simplification for the linear case in Ref. 32 and here we use the same approach to obtain the second-order susceptibility which relates the average polarization to the averaged fields.

C. Spatial symmetry of $\chi^{(2)}$

In bulk zinc-blende crystals, the symmetry properties of the electronic states at point Γ of the Brillouin zone are given by the tetrahedral point group T_d.[33] In a frame of references with axes x, y, z along the basic crystallographic directions [100], [010], and [001], this symmetry reduces the number of independent nonzero elements of $\chi^{(2)}$ to one. In the case of SQW's, the symmetry is reduced from T_d to D_{2d}.[34–36] Here there are three independent elements. When the specular symmetry plane (σ_h) is absent, as in the case of an AQW, the point group is C_{2v} and there are seven nonzero elements. The symmetry increases when one uses the Luttinger Hamiltonian for the valence band with the neglect of the small linear terms. Then for the bulk we have the O_h point group, for SQW's the D_{4h} point group, and for AQW's the C_{4v} group. Only four independent components of $\chi^{(2)}$ are permitted by the C_{4v} symmetry.

We list in Table I all the nonzero elements of $\chi^{(2)}$ for the different cases. Here the frame of references is chosen with the z axis along the growth direction and the axes x and y are rotated of an angle of 45° in their plane. In this case the correspondence with the basic crystalographic directions must be kept in mind in comparing different components (our $\chi^{(2)}_{xxz}$ corresponds to $\chi^{(2)}_{xyz}$ in the usual choice). In the envelope function approach, it turns out to be a good approximation to neglect the linear terms in the Luttinger Hamiltonian for the hole states, so that the symmetry is the D_{4h} for the symmetric quantum wells and the C_{4v} for asymmetric wells. In this case only the AQW's give a contribution to $\chi^{(2)}$ and in the case of second harmonic generation the constitutive equations of type (2) take the form

$$\begin{aligned} P_x^{(2)} &= \varepsilon_0 \chi^{(2)}_{xxz} E_x E_z, \\ P_y^{(2)} &= \varepsilon_0 \chi^{(2)}_{xxz} E_y E_z, \\ P_z^{(2)} &= \frac{\varepsilon_0}{2}\left[\chi^{(2)}_{zxx}\left(E_x^2+E_y^2\right) + \chi^{(2)}_{zzz} E_z^2\right]. \end{aligned} \quad (7)$$

The problem is then reduced to the computation of the three independent terms described above.

III. EIGENSTATES AND DIPOLE MATRIX ELEMENTS IN AN AQW

We consider two types of AQW excited states: electron-hole unbound pairs and bound (exciton) states.

TABLE I. Symmetry determined properties of the second-order susceptibility tensor in bulk material and quantum wells. In the upper half of the table the lack of inversion symmetry of the bulk material is included, while in the lower half of the table it is neglected. In the latter case only the AQW potential contributes to $\chi^{(2)}$. N.B. Quite frequently second harmonic coefficients $d_{p\mu}(\omega) = \chi^{(2)}_{pqr}(\omega,\omega)/2$ are labeled with only two indices (p and μ), the second one indicating the six symmetric combinations of the last two indices, for instance, $\chi^{(2)}_{xxz}(\omega,\omega)/2 = d_{15}(\omega)$.

Symmetry (Sample)	$\chi^{(2)}_{pqr} \neq 0$
T_d (Bulk)	$\chi^{(2)}_{xxz} = \chi^{(2)}_{xzx} = \chi^{(2)}_{zxx} = -\chi^{(2)}_{yyz} = -\chi^{(2)}_{yzy} = -\chi^{(2)}_{zyy}$
D_{2d} (SQW)	$\chi^{(2)}_{xxz} = -\chi^{(2)}_{yyz}$, $\chi^{(2)}_{zxx} = -\chi^{(2)}_{zyy}$, $\chi^{(2)}_{xzx} = -\chi^{(2)}_{yzy}$
C_{2v} (AQW)	$\chi^{(2)}_{zxx}$, $\chi^{(2)}_{zyy}$, $\chi^{(2)}_{xxz}$, $\chi^{(2)}_{yyz}$, $\chi^{(2)}_{xzx}$, $\chi^{(2)}_{yzy}$, $\chi^{(2)}_{zzz}$
O_h (Bulk)	0
D_{4h} (SQW)	0
C_{4v} (AQW)	$\chi^{(2)}_{xzx} = \chi^{(2)}_{zyy}$, $\chi^{(2)}_{xxz} = \chi^{(2)}_{yyz}$, $\chi^{(2)}_{xzx} = \chi^{(2)}_{yzy}$, $\chi^{(2)}_{zzz}$

To calculate them we use a two-band model based on the envelope function approximation,[37] described in Ref. 38 which considers the anisotropy of the effective masses in the kinetic energy and the dielectric mismatch in the Coulomb interaction.

To describe the continuum in the limits of the above approximation, we have to solve the one-particle equations for the envelope functions of the electrons $|i\rangle$ and of the holes $|j\rangle$,

$$H_c|i\rangle = E_i|i\rangle \ , \ H_\beta|j\rangle = E_j|j\rangle \ ,$$

$$i = 1,2,\ldots ; \ j = 1\beta, 2\beta \ldots ; \ \beta, = \mathrm{hh}, \mathrm{lh} . \quad (8)$$

Here H_c is the confinement Hamiltonian of an electron in the conduction band and analogously H_β is the corresponding Hamiltonian in the heavy- (β=hh) or the light-hole (β=lh) valence band. The one-electron wave functions are $\langle \boldsymbol{r}|i,\boldsymbol{k}_\parallel\rangle = u_0^c(\boldsymbol{r})\langle \boldsymbol{r}_\parallel|\boldsymbol{k}_\parallel\rangle\langle z|i\rangle$, where $u_0^c(\boldsymbol{r})$ is the conduction band Bloch function at point Γ and $\langle \boldsymbol{r}_\parallel|\boldsymbol{k}_\parallel\rangle = \exp(i\boldsymbol{k}_\parallel\cdot\boldsymbol{r}_\parallel)/\sqrt{S}$ is a plane-wave normalized on the AQW surface S, with an analogous expression for the valence states. The ground state wave function of the AQW as a whole $|0\rangle$ is given as an antisymmetrized product of the N electron wave functions, N being the total number of electrons taken into consideration. In the coordinate space $|\boldsymbol{R}_N\rangle = |\boldsymbol{r}_1,\boldsymbol{r}_2,\ldots,\boldsymbol{r}_\mu,\ldots,\boldsymbol{r}_N\rangle$, we write $\langle \boldsymbol{R}_N|0\rangle = A\left\{\prod_{\mu,j,\boldsymbol{k}_\parallel}\langle \boldsymbol{r}_\mu|j,\boldsymbol{k}_\parallel\rangle\right\}$. In a similar way, an excited state $|s\rangle$ is given by replacing one single valence state $|j,\boldsymbol{k}_\parallel\rangle$ by a conduction state $|i,\boldsymbol{k}'_\parallel\rangle$. We shall indicate it by the symbol $|i,\boldsymbol{k}'_\parallel,j,\boldsymbol{k}_\parallel\rangle$. On the other hand, the optical properties of bulk materials are characterized by the momentum matrix elements $|\langle u_0^c|\hat{p}_q|u_0^\beta\rangle| = \sqrt{E_K m_0/2}\, c_{q\beta}$, where E_K is the Kane energy (for GaAs $E_K \approx 23$ eV), m_0 is the electron mass, and the coefficients for heavy and light holes are $c_{x\mathrm{hh}} = 1/\sqrt{2}$, $c_{z\mathrm{hh}} = 0$, $c_{x\mathrm{lh}} = 1/\sqrt{6}$, and $c_{z\mathrm{lh}} = \sqrt{2/3}$.

We now follow the standard procedure[37,33] for calculating the dipole matrix elements from the ground state, using the momentum matrix elements, and we obtain

$$|\langle i,\boldsymbol{k}'_\parallel,j,\boldsymbol{k}_\parallel|\hat{d}_q|0\rangle|^2 = \delta_{\boldsymbol{k}_\parallel,\boldsymbol{k}'_\parallel}\frac{e^2\hbar^2E_K}{2m_0E_{ij}^2(k_\parallel)}c_{q\beta}^2\langle i|j\rangle^2 C_\beta(k_\parallel) . \quad (9)$$

Here $\langle i|j\rangle^2$ gives the confinement factor, the transition energy E_{ij} is given by $E_{ij}(\boldsymbol{k}_\parallel) = E_i - E_j + \epsilon(\boldsymbol{k}_\parallel)$, where ϵ is the kinetic energy $\epsilon(\boldsymbol{k}_\parallel) = \hbar^2\boldsymbol{k}_\parallel^{\,2}/2\mu_{ij}$, and μ_{ij} is the corresponding reduced mass. To take into account the residual Coulomb electron-hole interaction, we have included in the above matrix elements the so-called Coulomb enhancement factor[33,39,40] given by $C_\beta(k_\parallel) = \exp(\kappa\pi)/\cosh(\kappa\pi)$, where $\kappa = 1/k_\parallel a_b$ and $a_b = 4\pi\varepsilon_b\hbar^2/e^2\mu_\beta$ is the Bohr radius with a background dielectric constant ε_b.

For the dipole matrix elements among excited states we proceed in the same way as above and obtain with good approximation an expression which involves only the envelope functions

$$\langle i',\boldsymbol{k}'_\parallel;j',\boldsymbol{q}'_\parallel|d_z|i,\boldsymbol{k}_\parallel;j,\boldsymbol{q}_\parallel\rangle \simeq -e\delta_{\boldsymbol{k}_\parallel,\boldsymbol{k}'_\parallel}\delta_{\boldsymbol{q}_\parallel,\boldsymbol{q}'_\parallel}(\delta_{j,j'}\langle i'|z|i\rangle - \delta_{i,i'}\langle j'|z|j\rangle). \quad (10)$$

We would like to emphasize the fact that this dipole moment is different from zero for the AQW when $i = i'$ and $j = j'$ in Eq. (10), while it vanishes in case of SQW. This feature of the AQW's is the important element for explaining the strong rectification coefficients observed in the far infrared of doped samples.[1,5]

We also consider bound exciton states $|nS,i,j\rangle$ attached to a couple of of subbands i and j. These excited states can be expanded on the above described free electron-hole excited states[37] as $|nS,i,j\rangle = \sum_{\boldsymbol{k}_\parallel} A_{ij}^{nS}(\boldsymbol{k}_\parallel)|i,\boldsymbol{k}_\parallel,j,\boldsymbol{k}_\parallel\rangle$ and the envelope amplitudes $\varphi_{ij}^{nS}(\boldsymbol{r}_\parallel = \sum_{\boldsymbol{k}_\parallel} A_{ij}^{nS})(\boldsymbol{k}_\parallel)\langle \boldsymbol{r}_\parallel|\boldsymbol{k}_\parallel\rangle$ are obtained with a variational procedure using the expressions:[38,37]

$$\varphi_{ij}^{1S}(r_\parallel) = \sqrt{\frac{2}{\pi}}\frac{1}{\lambda_{ij}}\exp\left(-\frac{r_\parallel}{\lambda_{ij}}\right),$$
$$\varphi_{ij}^{2S}(r_\parallel) = \sqrt{\frac{2}{3\pi}}\frac{1}{3\lambda_{ij}}\left(1-\frac{2r_\parallel}{3\lambda_{ij}}\right)\exp\left(-\frac{r_\parallel}{3\lambda_{ij}}\right), \quad (11)$$

λ_{ij} being the effective exciton radius. We have taken the $2S$ exciton amplitude as a two-dimensional $2S$-like function orthogonal to the ground $1S$ state, the only variational parameter being the $1S$ exciton radius λ_{ij}. That is because the $2S$ exciton energy possesses a very smooth minimum as a function of λ_{ij} and hence the stronger requirement is that of orthogonality.

To derive the dipole matrix elements, we follow the same procedure as for the continuum, make use of the exciton wave packet, and obtain

$$|\langle nS,i,j|d_q|0\rangle|^2 = S\frac{e^2\hbar^2E_K}{2m_0E_{ij}^{nS\,2}}c_{q\beta}^2\langle i|j\rangle^2\left|\varphi_{ij}^{nS}(0)\right|^2, \quad (12)$$

where the exciton transition energy E_{ij}^{nS} is expressed by $E_{ij}^{nS} = E_i - E_j - R_{ij}^{nS}$, $R_{ij}^{nS} > 0$ being the exciton binding energy. It is worthwhile to note that the expression $\left|\varphi_{ij}^{nS}(0)\right|^2$ substitutes the $C_\beta(k_\parallel)$ in Eq. (9) with the continuum exciton amplitudes.[40] Analogously, we obtain the only nonzero exciton-exciton transition matrix elements $\langle nS,i',j'|d_z|nS,i,j\rangle$

$$= -4e\frac{\lambda_{i',j'}\lambda_{i,j}}{(\lambda_{i',j'}+\lambda_{i,j})^2}(1+\delta_{n,2}\Delta\lambda_{ij,i'j'}) \times\left(\delta_{j',j}\frac{E_{i'}-E_i+\delta_{i,i'}}{E_{i'j}^{nS}-E_{ij}^{nS}+\delta_{i,i'}}\langle i'|z|i\rangle - \delta_{i',i}\frac{E_{j'}-E_j+\delta_{j,j'}}{E_{ij'}^{nS}-E_{ij}^{nS}+\delta_{j,j'}}\langle j'|z|j\rangle\right), \quad (13)$$

where $\Delta\lambda_{ij,i'j'}$ is substituted to be

$$\Delta\lambda_{ij,i'j'} = 8\frac{\lambda_{ij}\lambda_{i'j'}}{(\lambda_{ij}+\lambda_{i'j'})^2} - 1 . \quad (14)$$

Thus as eigenstates $|s\rangle$ of an AQW we consider the continuum ($s \equiv i,j,\boldsymbol{k}_\parallel$) and the bound ($s \equiv n,i,j$)

exciton states and take into account transitions of the ground state–continuum, ground state–bound exciton state, continuum-continuum, and bound exciton–bound exciton types. We neglect transitions as bound-continuum exciton state because they give very little contribution to the nonlinear processes as in the case of SQW under an electric field.[10]

IV. SECOND-ORDER SUSCEPTIBILITY OF AN AQW

In the preceding section, we have shown how to describe different second-order optical phenomena in quantum wells. Let us now consider in details the process of second harmonic generation, described by $\chi^{(2)}_{pqr}(\omega,\omega)$, and use the abbreviated notation $\chi^{(2)}_{pqr}(\omega)$ or simply $\chi^{(2)}_{pqr}$ in our further considerations.

Substituting the dipole matrix elements in Eq. (3), we obtain an expression for $\chi^{(2)}$ in the form

$$\chi^{(2)}_{pqr}(\omega) = \sum_{i,j\neq j'} \kappa_{pqr}(i,i,j,j',\omega)\langle j|z|j'\rangle\langle j'|i\rangle\langle i|j\rangle - \sum_{j,i\neq i'} \kappa_{pqr}(i,i',j,j,\omega)\langle i|z|i'\rangle\langle i'|j\rangle\langle j|i\rangle - \sum_{i,j} \kappa_{pqr}(i,i,j,j,\omega) \times(\langle i|z|i\rangle - \langle j|z|j\rangle)\langle i|j\rangle^2 , \quad (15)$$

where κ_{pqr} denotes the resonant part, which consist of two terms

$$\hat{\kappa}^{(2)} = \hat{\kappa}^{(el)} + \hat{\kappa}^{(ex)} , \quad (16)$$

the continuum exciton contribution κ^{el} and the exciton contribution κ^{ex}. The first sum in Eq. (15) corresponds to the following types of precesses: valence band (j)–conduction band (i) and valence band–valence band (j'). Analogously, the second sum involves transition between two different conduction subbands (i,i') and one valence subband (j). These two terms have opposite signs and tend to cancel each other. This effect is stronger for the light holes because their effective mass in the z-direction is very closed to the electron mass (effect of cancellation). We should note that the confining potentials differ for holes and electrons. For example, in the case of strained InGaAs/GaAs QW's,[41] the light hole is weakly localized, while the electron is well confined in the QW, and hence the effect of cancellation should be much smaller than in more closely matched AQW's. The last term in Eq. (15) gives the contribution of virtual processes of a state with itself, which are typical of the AQW's.

A. Crossed component $\chi^{(2)}_{xxz}$

This component gives the polarization on the plane when the incident electric fields have both an in-plane and a z-component [Eqs. (7)]. Following the same procedure as above, we obtain, for the continuum contribution,

$$\kappa^{el}_{xxz}(i,i',j,j',\omega) = -K^{el}_{x\beta}\int d\epsilon \frac{C_\beta}{E_{ij}E_{i'j'}(\hbar\omega - E_{i'j'} + i\Gamma)(2\hbar\omega - E_{ij} + i\Gamma)}, \quad (17)$$

and for the exciton contribution

$$\kappa^{ex}_{xxz}(i,j,i',j',\omega) = \frac{-K^{ex}_{x\beta}}{(\lambda_{ij}+\lambda_{i'j'})^2}\sum_{n=1,2}\left[\frac{E_{ij}-E_{i'j'}+\delta_{i,i'}\delta_{j,j'}}{E^{nS}_{ij}-E^{nS}_{i'j'}+\delta_{i,i'}\delta_{j,j'}}\right]\frac{(\delta_{1,n}+\delta_{2,n}\Delta\lambda_{ij,i'j'}/27)}{E^{nS}_{ij}E^{nS}_{i'j'}(\hbar\omega - E^{nS}_{i'j'} + i\Gamma)(2\hbar\omega - E^{nS}_{ij} + i\Gamma)}. \quad (18)$$

Here we used the substitutions

$$K^{el}_{p\beta} = -\frac{e^3}{4\pi\epsilon_0 L_w}\frac{\mu_{r\beta}}{m_0}E_K {c_{p\beta}}^2, \qquad K^{ex}_{p\beta} = -\frac{4e^3\hbar^2}{\pi\epsilon_0 m_0 L_w}E_K {c_{p\beta}}^2, \quad (19)$$

where L_w is the AQW width and $c_{p\beta}$ are numerical coefficients given in Sec. III. Please note the small contribution of the $2S$ exciton states in Eq. (18), which is about 30 times smaller than the $1S$ contribution. In Eq. (17) we changed the summation on the in-plane vector $\boldsymbol{k}_{\|}$ with integration on the kinetic energy ϵ. We see that this component possesses simple resonances when $2\hbar\omega \approx E^{nS}_{ij}$. In this case, the incident wave spreads without absorption through the sample. On the other hand, there are also double resonance terms when $\hbar\omega \approx E_{ij}$ and $2\hbar\omega \approx E_{ij'}(E_{i'j})$, which could lead to extremely large peak values with respect to those expected near single resonances. In the widely used material GaAs/$Ga_{1-x}Al_xAs$, the double resonances are impossible because the confining potential is smaller than E_g. We show in Fig. 1 the spectrum of $\chi^{(2)}_{xxz}(\omega)$ for a typical steplike AQW, when the frequency of the incident electromagnetic wave is near half of the fundamental band gap (half-band-gap spectrum). In the calculations we have used the damping values (at $T = 4$ K) $\Gamma^{ex} = 2$ meV and $\Gamma^{el} = 4.7$ meV.[37,33,42] We see the manifestation of both direct (E_1HH_1, E_1LH_1, E_2HH_2,...) and indirect[38,43] (E_1HH_2, E_2LH_1, E_2HH_1,...) AQW excitons. The $2S$ excitons give a little contribution to the spectrum, but could be seen very clearly in the spectrum of the phase, where they appear as peaks near the corresponding $1S$ excitons.

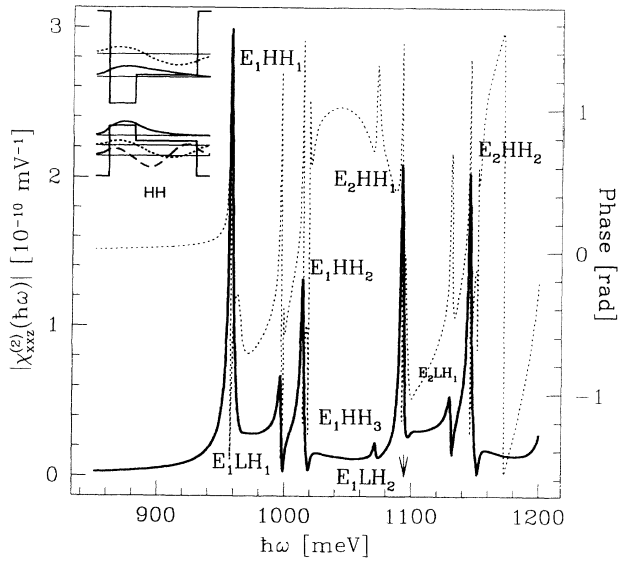

FIG. 1. Half-band-gap second-order susceptibility spectrum $\chi^{(2)}_{xxz}(\omega)$ for a steplike AQW composed of 1.5 nm GaAs and 3.5 nm $Ga_{0.6}Al_{0.4}As$ in a barrier region of AlAs. The electron and hole confining potentials are shown in the inset with the lowest electron and heavy-hole levels and the corresponding envelope functions. The solid line indicates $|\chi^{(2)}_{xxz}(\omega)|$ and refers to the left scale and the dotted line shows the phase expressed in radians on the right scale.

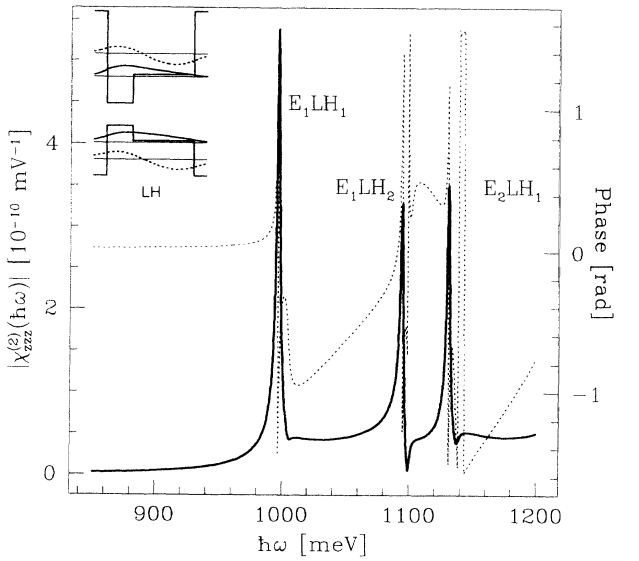

FIG. 2. Spectrum of the $\chi^{(2)}_{zzz}$ component for the same AQW as in Fig. 1 in the half-band-gap region. In the inset we show the lowest light-hole levels and envelope functions.

B. Perpendicular component $\chi^{(2)}_{zzz}$

As one sees from Eq. (7), this component gives the z polarization for an electromagnetic wave with electric field polarized along the z axis. This component is absent in the bulk case. The continuum electron contribution is

$$\kappa^{el}_{zzz}(i,i',j,j',\omega) = 2K^{el}_{z\beta}\int d\epsilon \frac{C_\beta}{E_{ij}E_{i'j'}(\hbar\omega - E_{ij} + i\Gamma)} \times \left(\frac{1}{\hbar\omega + E_{i'j'} + i\Gamma} - \frac{1}{2\hbar\omega - E_{i'j'} + i\Gamma}\right) \quad (20)$$

and the exciton contribution

$$\kappa^{ex}_{zzz}(i,i',j,j',\omega) = \frac{2K^{ex}_{z\beta}}{(\lambda_{ij}+\lambda_{i'j'})^2}\sum_{n=1,2}\left[\frac{E_{ij} - E_{i'j'} + \delta_{i,i'}\delta_{j,j'}}{E^{nS}_{ij} - E^{nS}_{i'j'} + \delta_{i,i'}\delta_{j,j'}}\right] \times \frac{(\delta_{1,n} + \delta_{2,n}\Delta\lambda_{ij,i'j'}/27)}{E^{nS}_{ij}E^{nS}_{i'j'}(\hbar\omega - E^{nS}_{ij} + i\Gamma)} \times \left(\frac{1}{\hbar\omega + E^{nS}_{i'j'} + i\Gamma} - \frac{1}{2\hbar\omega - E^{nS}_{i'j'} + i\Gamma}\right). \quad (21)$$

We see that this component possesses both single and double resonances and therefore gives the largest contribution to the polarization P_z, in spite of the fact that only light-hole excitons and interband transitions contribute to it. We wish to remark that this term has been erroneously neglected in previous papers. We present in Fig. 2 the plot of $\chi^{(2)}_{zzz}$ for the same AQW as in the previous case. We see that the light-hole peaks are of the same order of magnitude as the corresponding ones for the heavy holes in the $\chi^{(2)}_{xxz}$ spectrum. This may be explained with the fact that the effect of cancellation is compensated with the larger exciton binding energy[38] and light-hole dipole moment in the z direction ($c^2_{\mathrm{hh}x}/c^2_{\mathrm{lh}z} = 3/4$), as well as with the weaker cancellation between different exciton peaks, because of the relatively large distances.

C. In-plane component $\chi^{(2)}_{zxx}$

From expression (7) we can observe that the nonlinear polarization $P^{(2)}_z$ when the electric fields lie in the plane (x,y) of the AQW is determined by $\chi^{(2)}_{zxx}$. To calculate this term, we substitute the dipole matrix elements (9) and (10) into Eq. (3) and obtain

$$\kappa^{el}_{zxx}(i,i',j,j',\omega) = 2K^{el}_{x\beta}\int d\epsilon \frac{C_\beta}{E_{ij}E_{i'j'}(\hbar\omega - E_{ij} + i\Gamma)(\hbar\omega + E_{i'j'} + i\Gamma)}, \quad (22)$$

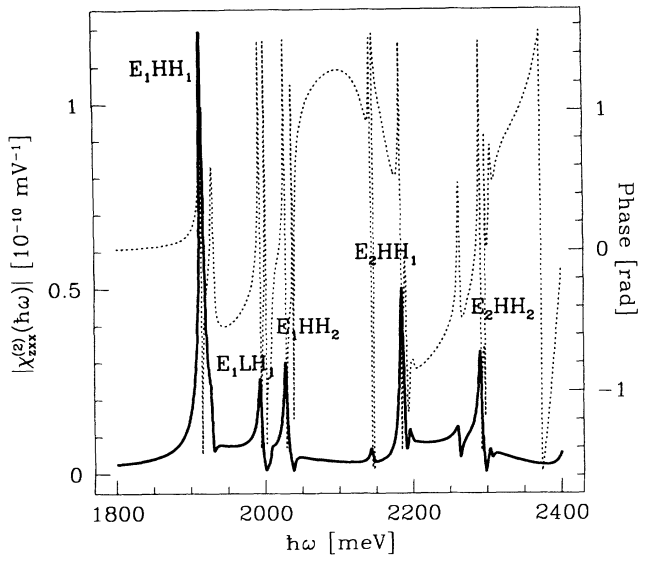

FIG. 3. Spectrum of the $\chi^{(2)}_{zxx}$ component for the same AQW as in Fig. 1 in a frequency region near the band gap.

and substituting expressions (12) and (13),

$$\kappa^{ex}_{zxx}(i,j,i',j',\omega) = \frac{2K^{ex}_{x\beta}}{(\lambda_{ij}+\lambda_{i'j'})^2}\sum_{n=1,2}\left[\frac{E_{ij}-E_{i'j'}+\delta_{i,i'}\delta_{j,j'}}{E^{nS}_{ij}-E^{nS}_{i'j'}+\delta_{i,i'}\delta_{j,j'}}\right] \times\frac{(\delta_{1,n}+\delta_{2,n}\Delta\lambda_{ij,i'j'}/27)}{E^{nS}_{ij}E^{nS}_{i'j'}(\hbar\omega-E^{nS}_{ij}+i\Gamma)(\hbar\omega+E^{nS}_{i'j'}+i\Gamma)}. \quad (23)$$

We see that this component of the second harmonic susceptibility possesses only single resonances in the region of the fundamental band gap E_g, when $\hbar\omega \approx E^{nS}_{ij}$: this occurs in correspondence to both heavy-hole and light-hole resonances. According to the interband dipole matrix elements ($c^2_{xlh}/c^2_{xhh}=1/3$) the peak values of the light-hole excitons are weaker than the heavy-hole ones. This can be seen in Fig. 3, where we have plotted $\chi^{(2)}_{zxx}(\omega)$ in the exciton (near-band-gap) region.

V. SECOND-ORDER SUSCEPTIBILITY WITH NONLOCAL INTERACTION

In this section we show how to calculate the second-order susceptibility, taking into account the nonlocality of the interaction between the electromagnetic field and the charge distribution inside a single AQW. In this case, we base our calculations on the fact that $\lambda \gg L_w$. As a first approximation, we can neglect the z component of the light wave vector $\boldsymbol{Q}$ inside the well and look for the average second-order susceptibility $\overline{\chi}^{(2)}$ defined by the relation

$$\overline{P}^{(2)}_p(2\omega) = \frac{\varepsilon_0}{2}\overline{\chi}^{(2)}_{pqr}(\omega,\omega)\overline{E}_q(\omega)\overline{E}_r(\omega). \quad (24)$$

A. Crossed component

We follow the procedure used in Ref. 32 for the linear case, and use a parallel $\varepsilon_{\parallel}(\omega)$ and perpendicular $\varepsilon_{\perp}(\omega)$ linear dielectric functions, whose expressions are also given in Ref. 32. We recall that the linear z component of the electric displacement vector $\boldsymbol{D}$ is given by

$$D_z(\omega) = \varepsilon_{\perp}(\omega)\overline{E}_z(\omega) \quad (25)$$

and is a constant inside the AQW. On the other hand, the perpendicular component E_z changes through the internal boundaries. It is given as a steplike function $E_z(z)$, which changes according to the usual boundary conditions.[32] It is worthwhile to note that because of the very large light wavelength λ in comparison with the AQW width L_w, the above statements remain valid for any direction of the incident wave, as well as in the case of multiple AQW's when the single period $L \ll \lambda$.

In our case, taking into account Eq. (7), we perform a space average in Eq. (5) for fixed indices $p = x$, $q = x$, and $r = z$, and obtain

$$\overline{P}^{(2)}_x(2\omega) = \varepsilon_0 L_w \sum_{i,i',j,j'}\kappa_{xxz}(i,j,i',j',\omega)\,\langle i|j\rangle\langle i'|j'\rangle\overline{E_x} \times\{\,\delta_{i,i'}\,\overline{[z\langle j'|z\rangle\langle z|j\rangle E_z(z)]} -\delta_{j,j'}\,\overline{[z\langle i'|z\rangle\langle z|i\rangle E_z(z)]}\,\}. \quad (26)$$

Here the resonant part $\kappa_{xxz}(i,j,i',j',\omega)$ is given by the same expression as obtained in Sec. IV. The contribution of the nonlocal interaction between the field and the well is given by the integrals $\langle z\langle k|z\rangle\langle z|l\rangle E_z(z)\rangle$, which can be calculated by expanding $P_z(z)$ to first order of the field as in the linear case. We make use of the linear constitutive equation[32]

$$E_z(z,\omega) = \varepsilon_b^{-1}(z)D_z - L_w\sum_{i,j}\chi^{(1)}_z(i,j,\omega)\langle i|z\rangle\langle z|j\rangle \times\varepsilon_b^{-1}(z)\langle\langle i|z\rangle\langle z|j\rangle E_z\rangle \quad (27)$$

to multiply by $Z_{kl}(z) = z\langle k|z\rangle\langle z|l\rangle$ and perform a space average on the both sides, to obtain

$$Z_{kl}(\omega) = \langle\varepsilon_b^{-1}Z_{kl}(z)\rangle - L_w\sum_{i,j}\chi^{(1)}_z(i,j,\omega) \times\langle\varepsilon_b^{-1}\langle i|z\rangle\langle z|j\rangle\, Z_{kl}(z)\rangle\zeta_{ij}(\omega), \quad (28)$$

where the functions

$$Z_{kl}(\omega) = \langle Z_{kl}(z)E_z(z)\rangle/D_z \quad (29)$$

depend only on the photon frequency ω since D_z is a constant across the interfaces. The couple of states k and l belong to the same band, while similar expressions,

$$\zeta_{ij}(\omega) = \langle\langle i|z\rangle\langle z|j\rangle E_z(z)\rangle D_z, \quad (30)$$

correspond to interband transitions and are given as solutions of the following system of equations:[32]

$$\sum_{i',j'}[\delta_{i,i'}\delta_{j,j'} + L_w\chi_z^{(1)}(i',j',\omega) \times\langle\varepsilon_b^{-1}\langle i'|z\rangle\langle z|j'\rangle\,\langle i|z\rangle\langle z|j\rangle\rangle]\zeta_{i'j'} = \langle\varepsilon_b^{-1}\langle i|z\rangle\langle z|j\rangle\rangle. \quad (31)$$

Computing the ζ_{ij} from (31) and substituting into (28) to obtain the Z_{kl} to be used in (29) and (25) and substituting the averages into Eq. (26) we finally obtain an equation of the type (24) where the second harmonic susceptibility is

$$\bar{\chi}^{(2)}_{xxz}(\omega) = \varepsilon_\perp(\omega)\sum_{i,i',j,j'}\kappa_{xxz}(i,j,i',j',\omega)\langle i|j\rangle\langle i'|j'\rangle \times[\delta_{i,i'}\,Z_{j,j'}(\omega) - \delta_{j,j'}\,Z_{i,i'}(\omega)]. \quad (32)$$

This is the expression which gives the second-order susceptibility $\bar{\chi}^{(2)}_{xxz}$ with inclusion of all nonhomogeneities due to the AQW structure and expressed in terms of the κ_{xxz} containing all the resonances, as described in Sec. IV. To compute it for all specific cases only requires a microscopic calculation of exciton and continuum states.

We show in Fig. 4 the plot of $|\bar{\chi}^{(2)}_{xxz}(\omega)|$ for a double AQW, in a frequency region near the fundamental band gap. We see that the effect of the nonlocal interaction decreases the stronger E_1HH_1 exciton peak and increases the light-hole exciton peaks whose resonances coincide with the $\varepsilon_\perp$ resonances. We may conclude that the nonhomogeneity in the z direction produces a small redistribution of spectral intensity from the heavy-hole peaks to the light-hole ones.

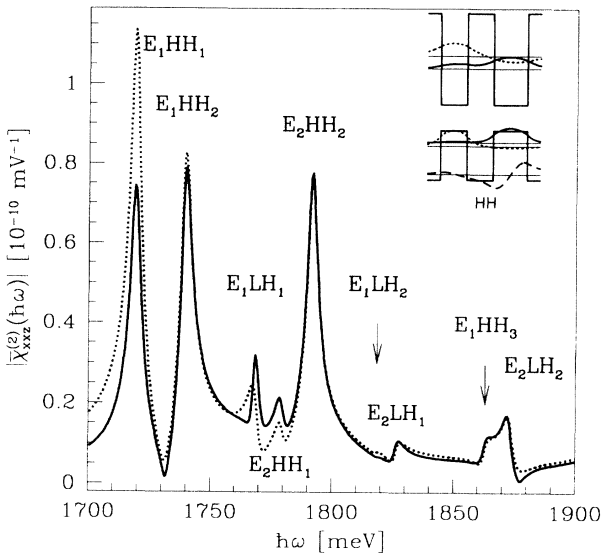

FIG. 4. Crossed quadratic susceptibility $|\bar{\chi}^{(2)}_{xxz}(\omega)|$ in the band-gap region calculated for the double AQW given in the inset and taking into account the internal nonhomogeneity of the well (solid line). The corresponding spectrum, without consideration of nonlocal effects, is shown by a dotted line. The AQW consists of $Ga_{0.5}Al_{0.5}As$ barrier regions and two GaAs wells of width 2.2 nm and 2.8 nm and separated by a 2.2 nm barrier. Electron and heavy-hole eigenstates are shown in the inset.

B. Perpendicular and in-plane component

We can repeat the same procedure for an electromagnetic wave polarized along the z axis to obtain

$$\bar{\chi}^{(2)}_{zzz}(\omega) = 4\varepsilon_\perp(\omega)^2\sum_{i,i'\ j,j'}\{\kappa_{zxx}(i,j,i',j',\omega)\,(\delta_{i,i'}\langle j|z|j'\rangle - \delta_{j,j'}\langle i|z|i'\rangle)\,\zeta_{ij}(\omega)\zeta_{i'j'}(\omega) + 2\,\kappa_{xxz}(i,j,i',j',E)\langle i|j\rangle\zeta_{i'j'}(\omega)\,[\delta_{i,i'}Z_{jj'}(\omega) - \delta_{j,j'}Z_{ii'}(\omega)]\}\ . \quad (33)$$

Here the resonant term κ_{zxx} is given by Eqs. (22) and (23) for the continuum and the exciton contribution, respectively, and analogously κ_{xxz} is given by Eqs. (17) and (18). The summation on j and j' is performed in this case on the light-hole states only (β=lh) because the dipole matrix elements vanish for the heavy hole in the z direction. In Fig. 5 we show the $|\bar{\chi}^{(2)}_{zzz}(\omega)|$ spectrum. We see that in this case the effect of the nonlocality of the interaction is to increase by more than 3 times the principal E_1LH_1 exciton peak. That is related to the fact that this peak coincides with the corresponding peak in the absorption spectra described by $\varepsilon_\perp$ (see Fig. 6).

For what concerns the component $\bar{\chi}^{(2)}_{zxx}$, we can use the same expressions as in Sec. IV because the in-plane components E_x, E_y do not change inside the AQW and nonlocal effects are not present in our approximation. We report the second harmonic spectrum calculations for the double AQW in the near-band-gap region in Fig. 6. Note the very clear presence of the crossed E_1HH_2 exciton transition, which is very weak in the linear absorption spectrum.

C. Contribution of the bulk and multiple AQW

In the preceding sections we have calculated the $\bar{\chi}^{(2)}$ of a single AQW taking into account the asymmetry of the confining potential and the internal inhomogeneity of the sample. We can observe that the maximum peak values previously computed are of the same order as those computed and measured in the bulk,[24–26] which may seem surprising because of the additional symmetry. In fact we have only considered the confining potential effect, as can be seen from the fact that our expressions so far do

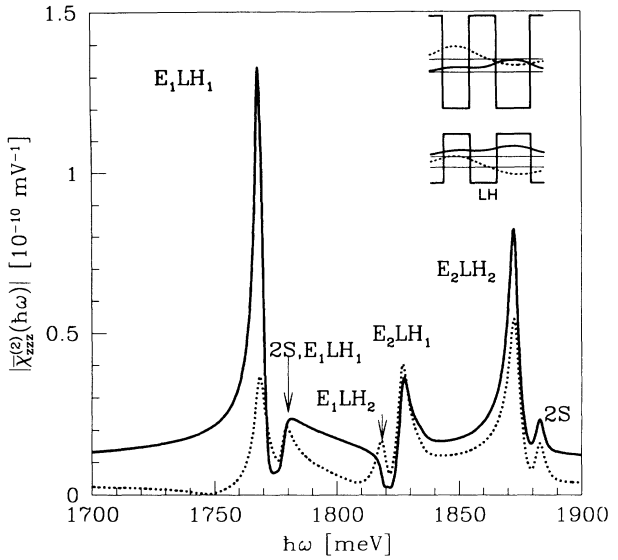

FIG. 5. Near-band-gap spectrum $|\bar{\chi}^{(2)}_{zzz}(\omega)|$ (solid line) and local $|\chi^{(2)}_{zzz}(\omega)|$ (dotted line) for the same AQW as in Fig. 4. Electron and light-hole confined states are shown in the inset.

not give the correct limit when $L_w \to \infty$, which should be the bulk value of $\chi^{(2)}$, as well as when we change smoothly the geometry of the AQW to the case of a symmetric QW, where $\bar{\chi}^{(2)} \to 0$. The reason is twofold: (i) we have adopted the first order envelope function approximation as described in Sec. III with symmetry C_{4v}, which corresponds to O_h and zero $\chi^{(2)}$ for the bulk, as shown in Table I, and (ii) we include only Γ_6 and Γ_8 bands and do not take into account the other conduction

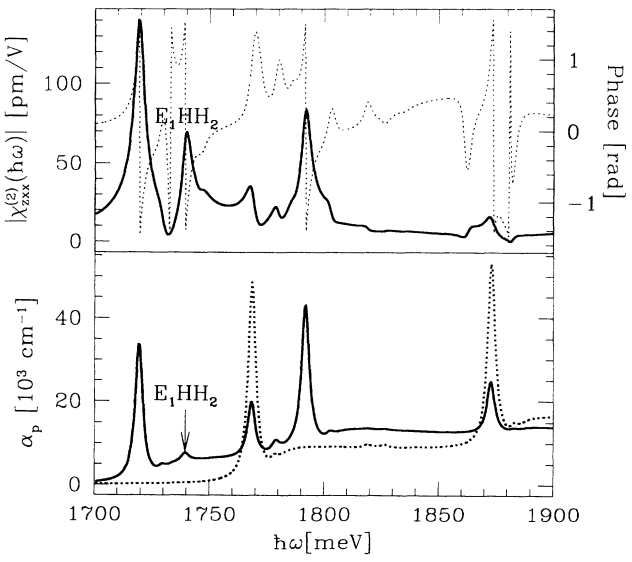

FIG. 6. Near-band-gap spectrum $|\chi^{(2)}_{zxx}(\omega)|$ for the same AQW as in Fig. 4. The dotted line is the phase given in radians on the right scale. In the lower part of the figure we show the absorption spectra $\alpha_p(\omega)$ when the incident electromagnetic wave is polarized along the x axis ($p = x$, solid line), as well as along the growth direction z (dotted line).

and valence bands of the bulk. In the linear case, the envelope function approximation does not introduce the above-mentioned problems because only interband matrix elements appear in that case, while for second-order processes intraband dipole matrix elements, as well as virtual transitions to all the bands, appear. To estimate the effect of the terms neglected in our approximation, we reconsider the momentum matrix element (related to the dipole one in the usual way) of the intraband type of expression (10)

$$\langle i,\boldsymbol{k},j\boldsymbol{k}|p_z|i',\boldsymbol{k},j'\boldsymbol{k}\rangle = [\delta_{jj'}\langle i|p_z|i'\rangle - \delta_{ii'}\langle j|p_z|j'\rangle] + \delta_{ii'}\delta_{jj'}[\langle u_{c\boldsymbol{k}}|p_z|u_{c\boldsymbol{k}}\rangle - \langle u_{\beta\boldsymbol{k}}|p_z|u_{\beta\boldsymbol{k}}\rangle], \quad (34)$$

where $u_{c\boldsymbol{k}}$ and $u_{\beta\boldsymbol{k}}$ are the Bloch function at some fixed $\boldsymbol{k}$ point. That is the expression that should be used in the calculation of the susceptibility. We see that the first two terms in Eq. (34) correspond to those we have used previously. They come from the confining AQW potential and do not relate to the bulk susceptibility. On the other hand, the third and fourth terms in Eq. (34) depend on the bulk band structure only and do not include contributions from the AQW potential. When we substitute them in Eq. (5) and expand the sum over all the bands, we obtain an additional term χ^b, which contributes to the total AQW susceptibility and goes to the susceptibility of the bulk when $L_w \to \infty$. In Eq. (5), the bulk matrix elements are multiplied by the oscillator strengths of the AQW excitons, and hence we may expect that χ^b is greater than or equal to the bulk susceptibility and possesses resonance peaks on the QW exciton energies. Note that because of its bulk origin χ^b gives a QW susceptibility even in the case of symmetric QW's as observed experimentally.[17] A complete calculation of this bulklike contribution is a rather difficult task because it requires the knowledge of the band structure, as modified by the quantum well. As a first approximation, which gives the correct limit at $L_w \to \infty$, we take as a value of χ^b to be added to the previous result the bulk susceptibility, as calculated by Moss *et al.*[25,26]

Another fact to consider is that we may have multiple quantum wells with barrier region of length $L_B = L - L_w$ and bulk susceptibility of the barrier χ^B. To take into account both the above described contributions we add to $\chi^{(2)}_{pqr}(z,z_1,z_2)$ of Eq. (4) the term

$$[\chi^B_{pqr}\Theta(z-L_w) + \chi^b_{pqr}(z)\Theta(L_w-z)] \times\delta(z-z_1)\delta(z-z_2), \quad (35)$$

where $\Theta(z)$ is the step function. Then we proceed in a similar way as for $\bar{\chi}^{(2)}$ and perform the space average on the period L. In this way, with simple algebraic manipulations, we obtain the following expressions:

$$\chi^{\mathrm{MQW}}_{zxx} = \frac{1}{L}\left(L_B\chi^B_{zxx} + \int_0^{L_w} dz\,\chi^b_{zxx} + L_w\bar{\chi}^{(2)}_{zxx}\right), \quad (36)$$

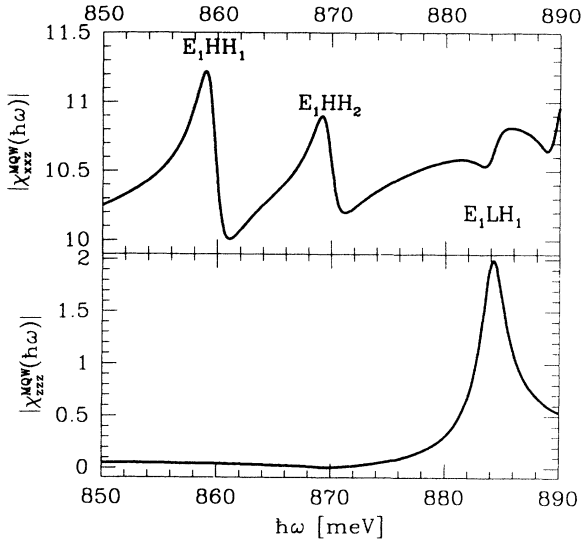

FIG. 7. Nonlinear $|\chi^{\mathrm{MQW}}_{xxz}(\omega)|$ (upper plot) and $|\chi^{\mathrm{MQW}}_{zzz}(\omega)|$ (lower plot) spectra for a multiple AQW consisting of AQW's as in Fig. 4, separated by barrier regions of width 3.8 nm. The vertical scales are given in units of 10^{-10} mV^{-1}.

$$\chi^{\mathrm{MQW}}_{xxz} = \frac{1}{L}\left(L_B \frac{\varepsilon_\perp}{\varepsilon_B}\chi^B_{zxx} + \varepsilon_\perp \int_0^{L_w} dz\, \frac{\chi^b_{xxz}}{\varepsilon_b} + L_w \overline{\chi}^{(2)}_{xxz} \right), \tag{37}$$

$$\chi^{\mathrm{MQW}}_{zzz} = \frac{1}{L}\left(L_B \frac{\varepsilon^2_\perp}{\varepsilon^2_B}\chi^B_{zzz} + \varepsilon^2_\perp \int_0^{L_w} dz\, \frac{\chi^b_{zzz}}{\varepsilon^2_b} + L_w \overline{\chi}^{(2)}_{zzz} \right), \tag{38}$$

where ε_B is the barrier dielectric function and χ^B is the barrier susceptibility; $\varepsilon_b(z)$ is the background dielectric function and χ^b is the second-order bulk susceptibility, both dependent on the alloy composition at point z of the well region; $\overline{\chi}^{(2)}_{pqr}$ is given by Eqs. (32), (33), (22), and (23).

With the above prescriptions we are now in a position to compute the second-order susceptibility of any multiple AQW, including both inversion asymmetry and confinement effects. The general result is to increase considerably the overall values of χ^{MQW} and to modify significantly its frequency dependence. We observe that, according to Table I, the barrier and bulk contribution to $\chi^{\mathrm{MQW}}_{zzz}$ vanish by symmetry so that for this tensor component the results of Sec. V B are not modified.

As an illustrative example we give in Fig. 7 the frequency dependence of $|\chi^{\mathrm{MQW}}_{xxz}|$ and $|\chi^{\mathrm{MQW}}_{zzz}|$ up to the half-band-gap region, having used for the bulk and barrier susceptibilities the values computed by Moss *et al.*[25,26] It can be noticed that the basic structure due to the confinement potential asymmetry is preserved and peaks corresponding to all QW excitons can be observed, though their line shape is much more asymmetric than without the bulk contribution and all the frequency-dependent values are consistently increased. This is in basic agreement with the experimental observations reported in Ref. 17.

In the present self-consistent calculation of $\overline{P}^{(2)}$ we have not included contributions which originate from the linear response of the type

$$\delta \boldsymbol{P}^{(2)}(2\omega) = \varepsilon_0 \hat{\chi}^{(1)}(2\omega)\boldsymbol{E}(2\omega), \tag{39}$$

where $\boldsymbol{E}(2\omega)$ is the field produced by second harmonic generation. The requirement of self-consistency gives a small correction to our results, which may be relevant in different materials. This question will be considered in another paper.

The above described theory allows a reasonably good understanding of the overall microscopic processes of second harmonic generation. Its weakest point is the fact that we must limit the summation on intermediate states and completeness cannot be ensured. This is particularly relevant also to satisfy the condition of gauge invariance when the scalar $(-\boldsymbol{d}\cdot\boldsymbol{E})$ or vector $(-\boldsymbol{p}\cdot\boldsymbol{A})$ potential representation are adopted. A way to improve on the above shortcoming is to impose that the sum rules are obeyed, as shown in Ref. 44 for $\chi^{(3)}$ of the hydrogen atom. We are currently investigating this possibility, making use of a set of newly derived sum rules.[45]

VI. CONCLUSIONS

The results of the above paper can be summarized as follows.

All the nonzero independent second-order susceptibility tensor components have been computed for a single and multiple AQW of arbitrary shape.

Contributions that go beyond the local approximation are shown to originate from the asymmetry of the confining potential. Other contributions originate from the inversion asymmetry of the material; they are responsible for the correct limits as $L_w \to \infty$ and AQW$\to$ SQW.

The spectral dependence of $\chi^{(2)}_{pqr}$ reflects the exciton structure with peaks of $\chi^{(2)}_{xxz}$ and $\chi^{(2)}_{zzz}$ at half band gap and of $\chi^{(2)}_{zxx}$ in the near-band-gap region. The contribution from the continuum states is relatively small in comparison with the exciton contribution.

The contribution of the inversion asymmetry and of the confining potential asymmetry reinforce each other in the case of $\chi^{(2)}_{xxz}$ and $\chi^{(2)}_{zxx}$, so that the susceptibility values are larger than those of the bulk. In particular $\chi^{(2)}_{zzz}$ is different from zero in AQW and originates from the well potential structure only.

ACKNOWLEDGMENTS

The authors are indebted to P. Giannozzi for his help in the numerical calculations. Thanks are also due to C. Andreani and G. La Rocca for the very useful and constructive discussions of this work.

[1] P. Bois, E. Rosencher, J. Nagle, E. Martinet, P. Boucaud, F.H. Juluen, D.D. Yang, and J.-M. Lourtioz, Superlatt. Microstruct. **8**, 369 (1990).
[2] P. Boucoud and F. Julien, J. Phys. (Paris) III **1**, 13 (1991).
[3] P. Boucaud, F.H. Julien, D.D. Yang, J-M. Lourtioz, E. Rosencher, P. Bois, and J. Nagle, Appl. Phys. Lett. **57**, 215 (1990).
[4] S. Yoo, M. Fejer, R. Byer, and J. Harris, Appl. Phys. Lett. **58**, 1724 (1991).
[5] E. Rosencher and P. Bois, Phys. Rev. B **44**, 11 315 (1991).
[6] P. Boucaud, F.H. Julien, D.D. Yang, E. Rosencher, and P. Bois, Opt. Lett. **16**, 199 (1991).
[7] C. Sirtori, F. Capasso, D. Sivco, S. Chu, and A. Cho, Appl. Phys. Lett. **59**, 2302 (1991).
[8] C. Sirtori, F. Capasso, D. Sivco, A. Hutchinson, and A. Cho, Appl. Phys. Lett. **60**, 151 (1992).
[9] M. Fejer, S. Yoo, R. Byer, A. Harwit, and J. Harris, Phys. Rev. Lett. **62**, 1041 (1989).
[10] L. Tsang, Sh. Chung, and Sh. Lee, Phys. Rev. B **41**, 5942 (1990).
[11] L. Tsang and S. Chuang, Phys. Rev. B **42**, 5229 (1990).
[12] J. Kurgin, Phys. Rev. B **38**, 4056 (1988).
[13] J. Kurgin, Appl. Phys. Lett. **51**, 2100 (1987).
[14] Y. Xie, Z. Chen, D. Cui, S. Pan, D. Deng, Y. Zhou, H. Lu, Y. Huang, S. Feng, and G. Yang, Phys. Rev. B **43**, 12 477 (1991).
[15] P. Harshman and S. Wang, Appl. Phys. Lett. **60**, 1277 (1992).
[16] S. Scandolo, A. Baldereschi, and F. Capasso, Appl. Phys. Lett. **62**, 3138 (1993).
[17] Zheng-hao Chen, Yuan-lin Xie, Shi-jie Gu, Yue-liang Zhou, Da-fu Cui, Hui-ben Lu, Jun-ming Zhou, Zu-yan Xu, and Guo-zhen Yang, Phys. Rev. B **42**, 5117 (1990).
[18] C. Sirtori, F. Capasso, D. Sivco, S. Chu, and A. Cho, Phys. Rev. Lett. **68**, 1010 (1992).
[19] W. Bloss and L. Friedman, Appl. Phys. Lett. **41**, 1023 (1982).
[20] C. Cooperman, L. Friedman, and W. Bloss, Appl. Phys. Lett. **44**, 977 (1982).
[21] D. Chemla and D. Miller, J. Opt. Soc. Am. B **2**, 1155 (1985).
[22] T. Wood, R. Tkach, and A. Chapllyvy, Appl. Phys. Lett. **50**, 798 (1987).
[23] D.E. Aspnes, Phys. Rev. B **6**, 4648 (1972).
[24] B.F. Levine and G.G. Betha, Appl. Phys. Lett. **20**, 272 (1972).
[25] D.J. Moss, J.E. Sipe, and H.M. van Driel, Phys. Rev. B **36**, 1153 (1987).
[26] D.J. Moss, J.E. Sipe, and H.M. van Driel, Phys. Rev. B **36**, 9708 (1987).
[27] Paul N. Butcher and David Cotter, *The Elements of Nonlinear Optics* (Cambridge University Press, Cambridge, 1990).
[28] J. Ducuing and C. Flitzanis, in *Optical Properties of Solids,* edited by F. Abelès (North-Holland, Amsterdam, 1972).
[29] V.M. Agranovich, in *Modern Problems in Condensed Matter Physics*, edited by V. Agranovich and D. Mills (North-Holland, Amsterdam, 1982), Vol. 1.
[30] V. Agranovich, Solid State Commun. **78**, 747 (1991).
[31] V. Agranovich and V. Kravtsov, Solid State Commun. **55**, 85 (1985).
[32] R. Atanasov, F. Bassani, and V.M. Agranovich, Phys. Rev. B **49**, 2658 (1994).
[33] F.G. Bassani and G.P. Parravicini, *Electronic States and Optical Properties in Solids*, edited by R.A. Ballinger (Pergamon Press, Oxford, 1975).
[34] V.M. Agranovich and V. Ginzburg, *Crystal Optics with Spatial Dispersion and Excitons* (Springer-Verlag, Berlin, 1984).
[35] L. Andreani, F. Bassani, and A. Pasquarello, in *Symmetry in Nature* (Scuola Normale Superiore, Pisa, 1991), p. 19.
[36] S. Jorda and U. Rössler, Superlatt. Microstruct. **8**, 481 (1990).
[37] G. Bastard, *Wave Mechanics Applied to Semiconductor Structures* (Les Editions de Physique CNRS, Paris, 1988).
[38] R. Atanasov and F. Bassani, Solid State Commun. **84**, 71 (1992).
[39] M. Shinada and S. Sugano, J. Phys. Soc. Jpn. **21**, 1936 (1966).
[40] P. Lefebvre, P. Christol, and H. Mathieu (unpublished).
[41] M.J. Joyes, Superlatt. Microstruct. **12**, 293 (1992).
[42] J. Martinez-Pastor, A. Vinattieri, L. Carraresi, M. Coloci, Ph. Roussignol, and G. Weimann, Phys. Rev. B **47**, 10 456 (1993).
[43] A. Zrenner, P. Leeb, J. Schafer, G. Weimann, J.M. Worlock, L.J. Florez, and J.P. Harbison, Surf. Sci. **263**, 496 (1992).
[44] S. Scandolo and F. Bassani, Nuovo Cimento D **14**, 873 (1992).
[45] S. Scandolo (private communication).